Hindawi
Advances in Civil Engineering
Volume 2023, Article ID 8881333, 17 pages
https://doi.org/10.1155/2023/8881333

Research Article

Analysis of Fouling Pattern of Tunnel Drainage Pipe in Karst Areas

Jianbing Lv,[1] **Hao Wu**,[1] **Jia Li**,[2] **Xiaodong Wan**,[1] **and Helin Fu**[1]

[1]*School of Civil and Transportation Engineering, Guangdong University of Technology, Guangzhou 510000, China*
[2]*Jiangmen Yinzhou Lake Expressway Co, Jiangmen 529152, China*

Correspondence should be addressed to Jianbing Lv; ljb@gdut.edu.cn

Received 10 May 2023; Revised 12 July 2023; Accepted 25 August 2023; Published 15 September 2023

Academic Editor: Ma Jianjun

As the groundwater in karst areas is rich in calcium ions, when the groundwater flows out of the tunnel drainage pipe, calcium carbonate crystals will be precipitated and then adhere to the pipe wall, which will easily cause chemical blockage in the drainage pipe wall, thus affecting the drainage efficiency and leading to the increase of water pressure outside the tunnel lining, affecting the safety and stability of the structure. Therefore, the blockage of calcium carbonate crystals in tunnel drains is one of the most important problems for the safe and normal operation of tunnels. In order to quantify and qualify the process of crystalline blockage in the drainage system of tunnels in karst areas, this paper constructs a numerical model with coupled multiphysical fields of the flow field and particle concentration field and also combines data from indoor tests to compare and verify the simulation results and analyze the time-varying law of crystalline solids deposited on the pipe wall. In this paper, we consider the force situation of crystalline solids in the pipe by water flow, analyze the related theories, comprehensively study the migration and deposition law of crystalline particles in the drainage pipe, and establish a numerical simulation model of the pipe crystallization rate considering temperature, flow velocity and concentration of sediment particles based on ANSYS FLUENT software, and refine and analyze several parameters in the model, so that it can provide a theoretical analysis framework for the tunnel drainage pipe blockage in karst areas by providing a theoretical analysis framework.

1. Introduction

In the process of operation and maintenance management of highway projects, the maintenance treatment technology for tunnels under complex engineering and hydrological geological conditions is very difficult, and the effect after maintenance treatment is poor. The high mineralization of groundwater in the aquifer in karst areas infiltrates into the drainage pipe, which leads to the crystallization of seepage water, thus blocking the drainage pipe due to the change in temperature and pressure conditions. The blockage or failure of drainage holes will jeopardize the stability and traffic safety of highway tunnels. Many scholars are exploring their efforts to solve the drainage hole blockage or intelligent detection [1]. The drainage pipe of the tunnel operating in karst areas is severely blocked by chemical crystallization [2], and the crystallization blockage leads to the poor drainage of the tunnel structure, which is extremely unfavorable to the safety of tunnel operation after the safety and stability coefficient of the tunnel structure is reduced with the extension of the operation time, and the safety hazards generated, the safety risks are increasing year by year. The factors affecting the clogging of tunnel drainage systems are complex [3], and it has been the goal of many researchers to develop a fine and realistic picture of the crystallization process of drainage pipes by using numerical models. Mullin proposed the adsorption layer model of the kinetic mechanism of calcite dissolution [4], which laid the foundation for chemical numerical analysis; Berner conducted experiments on the kinetic process of calcium carbonate dissolution in natural water, which revealed the mass transport diffusion mechanism in the dissolution process and chemical analysis. In the 1970s, the PWP (Plummer–Wigley–Parkhurst) model of calcite dissolution and deposition kinetics was proposed, taking into account the mobility conditions of the system, which summarized the kinetic mechanism of the dissolution surface of carbonate minerals in a more systematic way [5]; in the mid-1990s,

Oddo and Tomson integrated the thermodynamic, thermal, and sedimentation kinetics of calcite dissolution. Tomson integrated thermodynamics, ionic strength, solubility product, and ionic association theories to develop a predictive model capable of predicting the scaling trends of a wide range of scale salts based on the saturation index applicable to different cases of temperature and pressure [6]. More and more numerical models of ion chemistry and thermodynamics are being developed, making it possible to use computers to construct physicochemical reaction fields to analyze changes in the transport laws of substances.

Due to the limitations of various theoretical models for predicting carbonate chemical scaling trends, with the development of computer technology as well as numerical simulation, there is an increasing desire for software that can perform scaling trend prediction to optimize practical engineering. Brahim simulated the crystallization blockage process in a heat exchanger and explored the effect of different flow rates, concentrations, temperatures, pressures, and pipe wall materials on crystallization [5, 7]. Nergaard et al. [8] investigated the formation of a calcium carbonate scale on the outer surface of a heating pipe in a recirculation device, separated the influence of saturation from temperature, and analyzed the linear scale growth rate of the calcium carbonate scale [9]. Chi et al. [10] applied the groundwater chemistry simulation software Phreeqc to investigate the effect of temperature on the erosion of feldspar by groundwater solutions at different CO_2 partial pressures, calcium feldspar, potassium feldspar, and sodium feldspar in solution simultaneously and separately at different CO_2 partial pressures were hydrochemically simulated by Phreeqc [11]. Fang et al. [9] used a coupled computational fluid dynamics (CFD)-discrete element method to numerically analyze the movement of particles in a fractured fog model to clarify the migration and channel flow control law of particles in fractured porous carbonate reservoirs [12]; de Paula Cosmo et al. [11] analyzed the calcium carbonate fouling law in oil and gas field pipeline with high CO_2 content under pseudo-equilibrium conditions by self-developed thermodynamic calculation software [13]; Zhiming et al. [12] established a mathematical model of $CaSO_4$ precipitation fouling formation process in circular pipe from the perspective of heat and mass transfer, and conducted corresponding numerical simulation and experimental validation. Based on the simulated temperature, velocity, and $CaSO_4$ mass concentration fields in the circular pipe, the deposition rate, exfoliation rate, and thermal resistance of $CaSO_4$ fouling with time were calculated from this fouling model [14]. Liu et al. [13] innovatively combined electrochemical technology and quartz crystal microbalance with dissipation monitoring (QCM-D) in one analytical instrument (EQCM-D). EQCM-D to monitor $CaCO_3$ deposition in real time and provide kinetic details of the $CaCO_3$ deposition process [15]; Chen et al. [14] proposed an integrated thermodynamic model based on the electrolyte nonrandom double liquid activity coefficient equation for analytically accurate calculations of calcium carbonate scaling in high-salinity aquatic waters [16]. Ojaniemi et al. [15] developed a CFD model, which takes into account the precipitation tendency of fluid components and the surface properties of materials for calcium phosphate scaling; Ojaniemi et al. [15] developed a CFD model, which takes into account the precipitation tendency of fluid components and the surface properties of materials for calcium phosphate scaling; Ojaniemi et al. [15] developed a CFD model that takes into account the precipitation tendency of fluid components and the surface properties of materials for calcium phosphate scaling; Ojaniemi et al. [15] developed a CFD model that can simulate the precipitation of insoluble minerals due to elevated temperature in the near-surface region of the heated wall based on the saturation ratio. This preliminary CFD model of adhesion paves the way for the construction of a more comprehensive model [17]. Guanying and Jixiang [16] developed a time-varying model of divalent calcium ion concentration under each type and used PHREEQC software to solve the model to quantitatively resolve the source of divalent calcium ions in aqueous solution under the interaction of water, rock, and curtain [18]. Zhao et al. [17] designed a leachate pipe fouling experiment to simulate leachate fouling in a straight pipe and a 90° bend, investigated the characteristics of scale deposition changes in different pipe types, and analyzed the effects of temperature, flow rate, pipe wall roughness, scale particle size, and other factors on scale deposition [19]. Lü et al. [18] designed an experimental setup using FLUENT software to study the mechanism of scale deposition at different flow rates and different locations in a 90° bend [20]. Ma et al. [21, 22] built a thermo-elastic-plastic-damage coupling model of concrete using a thermodynamic framework, which can effectively capture the thermodynamic distribution of boundary surfaces. Xu et al. [23] studied the effects of water flow rate, drainage slope, and material contact Angle on pipe-to-pipe crystallization through model tests and proposed a crystallization quality prediction formula based on the test results. Zhou et al. [24] explored the influence of hydrodynamic factors on the development of pipeline crystallization and precipitation and designed a model test with hydrodynamic factors as observed variables. Feng et al. [25] designed a simulation test on the crystallization of drainage pipes with water temperature changes. According to the microscopic analysis of the test results, it was found that the morphology of crystals at different temperatures was different, and the amount of crystallization inside the pipes was the largest when the water temperature was about 45°. The numerical modeling of pipe fouling processes has been progressively refined through breakthroughs in CFD technology and thermodynamic analysis to the point where we can now attempt to apply it to tunnel drainage systems in karst areas.

In this paper, we first analyze the causes of calcium carbonate crystallization, then describe the force of calcium carbonate particles, transition the scaling process in the pipe from qualitative research to quantitative research, and finally introduce the numerical model to summarize the law of its blockage project, and quantitatively describe the whole process of crystallization and blockage inside the tunnel drainage pipe. The whole process of clogging is described quantitatively. The modeling method integrates fluid mechanics, particle kinematics, and other concepts to simulate a more accurate calcium

carbonate fouling process, which can provide a methodology to accurately determine the optimal maintenance and crystal breaking time nodes of drainage pipes.

2. Theory of Fouling in Tunnel Drainage Pipes in Karst Areas

2.1. Calcium Carbonate Precipitation Crystallization Scaling Mechanism. In natural groundwater, the nucleation process generally occurs in a saturated solution; there are many solid substrates such as fine silica sand particles, heterogeneous nucleation, and as a nucleus, calcium carbonate grains began to grow, forming inorganic ion oligomeric calcium carbonate particles of approximately 1.2 nm in size, with the free calcium ions and carbonate ions continue to join, the nucleus in the fluid movement will occur mutual with the continuous addition of free calcium ions and carbonate ions, the nucleation process shows a nonuniform trend as the grains become larger and larger, i.e., crystal adhesion process. The whole nucleation induction time consists of three stages: relaxation stage, nucleation stage, and growth stage. Supersaturation is a necessary condition to ensure that the whole crystallization process continues continuously. When the saturation in the solution is exhausted, the driving force of the crystallization process disappears, and the crystallization stops while the whole solid–liquid system regains equilibrium. It is generally believed that the scale formation process of the calcium carbonate scale is mainly composed of the following parts: supersaturation-nucleation-aggregation-crystal growth-scaling, which belongs to crystallization scale formation in the scale formation mode. When the number of crystals reaches a certain level, it starts to adhere to the tube wall and form a tube crystalline scale.

In addition, the water flow in the pipe is in continuous motion, and due to the viscous shear of the boundary layer, the water flow has a stripping effect on the deposited crystalline scale, which can be generalized as the stripping process of the calcium carbonate crystalline scale.

According to domestic and international literature, the formation process of calcium carbonate pipe scale can be summarized into the following four stages: initiation, transport, adhesion, and exfoliation [26]. The initiation stage refers to the contact between the fluid and the surface of calcium carbonate grains in the pipe until the formation of a microscale layer that can be observed with the naked eye and the duration of this process is difficult to estimate, ranging from a few hours to a few days. The transport stage is the transfer of calcium carbonate particles from the fluid to the pipe surface, where Brownian motion, molecular diffusion, applied force field (gravity, magnetic force, etc.), heat transfer convection, collision probability, etc., have a key influence on this process. The attachment stage is the main stage of the gradual thickening of the scale layer when the calcium carbonate particles near the pipe wall are captured by the wall and adsorbed on it; the exploitation stage mainly has three forms: dissolution, abrasion, and flaking [27], when the fluid is in a nonsaturated state, the scale layer will be dissolved again in the solvent in the form of ions, this is dissolution, or due to the continuous flow of fluid in the pipe, under the impact of water molecules and other kinetic energy of calcium carbonate particles, the scale layer already attached to the pipe wall will be washed away in the form of particles or blocks, the former is abrasion, the latter is flaking.

When the calcium carbonate particulate matter migrates from the middle of the fluid to the wall of the pipe, the diffusion equation of the particulate matter is as follows [28]:

$$\frac{dm'_{\mathrm{p}}}{dt} = K_t\left(c_{\mathrm{pb}} - c_{\mathrm{pw}}\right), \tag{1}$$

where $\frac{dm'_{\mathrm{p}}}{dt}$ is the rate of change of the mass of particles per unit time, K_t is the transport coefficient, c_{pb} is the concentration of the particle phase in the solution, and c_{pw} is the concentration of the particle phase at the wall.

Introduction of dimensionless ion relaxation times for particle transport τ_p^+ and transport coefficients K_t^*.

$$\tau_{\mathrm{p}}^+ = \frac{\tau_{\mathrm{p}}(V^*)^2}{\nu}, \tag{2}$$

$$\tau_{\mathrm{p}} = \frac{\rho_{\mathrm{p}} d_{\mathrm{p}}^2}{18\rho\nu}, \tag{3}$$

$$V^* = \sqrt{\tau_{\mathrm{w}}/\rho}, \tag{4}$$

$$K_{\mathrm{t}}^* = K_{\mathrm{t}}/V^*, \tag{5}$$

where V^* is the friction velocity, ν is the kinematic viscosity, τ_p is the time of the particle phase relaxation, τ_w is the shear force of the fluid, ρ and ρ_{p} are the densities of the fluid and the particle phases, respectively.

Calcium carbonate particles reach the wall of the pipe in a manner closely related to the size of the relaxation time; if it is greater than 10, the particles will collide with the wall of the pipe; if it is greater than 0.1, less than 10, the particles reach the wall due to inertia, if it is less than 0.1, the particles arrive due to mass transfer diffusion. If the viscosity of a very small fluid (such as water, air, etc.) is in contact with the object at large Reynolds number and relative motion, the thin fluid layer near the surface of the object due to viscous shear stress and reduce the speed; near the surface of the fluid adhered to the surface of the object, and the relative speed of the surface of the object is equal to zero; from the object upward, the speed of the layers gradually increased until equal to the free flow rate. Liquid flow in the drainage pipe mainly exists in the laminar boundary layer and turbulent boundary layer; the fluid velocity distribution from the mainstream area starting closer to the wall of the boundary layer water velocity is smaller and smaller until it is zero [29, 30]. When the calcium carbonate particles through the boundary layer to reach the pipe wall, before the wall can be attracted to attach, but not all particles will be adsorbed to form a crystalline scale; part of the kinetic energy is too large and rebound at this time the deposition coefficient is not equal to the transport coefficient, you need to consider the probability of collision Buddha attachment [31].

$$K_d = PK_t. \tag{6}$$

Pipe wall adhesion to particulate matter is controlled by many forces, such as wall conditions, particle diameter, fluid physical parameters, temperature, etc. According to the micromechanics theory, the source of the adsorption force of pipe wall on particulate matter consists of van der Waals force (intermolecular force), electrostatic gravitational force, and magnetic field gravitational force, which are all long-range forces and increase rapidly with distance, so the closer the particulate matter is to the wall, the greater the probability of being adsorbed. And some of the crystal particles colliding with the pipe wall will generate rebound force, i.e., short-range force, and the particles will be adsorbed only when the effect of the long-range force is greater than the short-range force.

The above scaling process has an exfoliation phase, so the exfoliation rate must also be introduced, and according to the net deposition model proposed by Kern and Seaton [30], the net deposition rate of the particulate matter can be calculated.

$$m = m_d - m_r, \tag{7}$$

where m is the net deposition rate of particulate matter, m_d is the deposition rate, m_r is the denudation rate.

$$m_\Delta = \beta\left\{\frac{1}{2}\frac{\beta}{k_s} + \Delta c - \left[\frac{1}{4}\left(\frac{\beta}{k_s}\right)^2 + \frac{\beta}{k_s}\cdot\Delta c\right]^{\frac{1}{2}}\right\}, \tag{8}$$

where m_Δ is the deposition rate; β is the convective mass transfer coefficient; k_s is the surface reaction rate constant, mainly related to the concentration of reactants, Δc is the concentration gradient of $CaCO_3$ in the pipe. The fouling stripping model is adopted from the model proposed by Bohnet [31]:

$$m_r = 0.012u^{1.46}m_f\left[1 + \beta\left(T_w - T_f\right)\right]d_P \times (\rho^2\mu g)^{\frac{1}{3}}, \tag{9}$$

where m_r is the stripping rate; u is the flow rate; m_f is the fouling mass per unit area; β is the linear expansion coefficient; T_w and T_f are the pipe wall temperature and fluid temperature, respectively; d_P is the crystal size.

2.2. Calcium Carbonate Precipitation Crystallization Scaling Mechanism. Calcium carbonate particles in the fluid migration movement or deposition down or not are ultimately determined by their force, the individual tiny particles for force analysis, identify the source of different forces, factors affecting the size, direction of action, the scope of action, etc., can be obtained from the trajectory of the particles and the law of motion. In the classical theory of fluid mechanics, it is generally believed that the particles in a fluid are mainly subjected to the following forces.

2.2.1. Gravity and Buoyancy. The calcium carbonate particles in the fluid in the discharge pipe are always subject to gravity and buoyancy. Assuming that the particles are all standard spheres, the gravitational and buoyant forces are calculated as follows:

$$F_g = \frac{1}{6}\pi d_p^3\rho_p g, \tag{10}$$

$$F_b = \frac{1}{6}\pi d_p^3\rho g, \tag{11}$$

where d_P is the particle size, ρ_P is the particle density, ρ is the density of water.

2.2.2. Inertia Force. When an object has acceleration, the object's inertia will cause the object to maintain its original state of motion, and the object of study is usually used as the reference system and establish the coordinate system on this reference system, as the Lagrangian method must be introduced in the subsequent study to describe the trajectory of particles, the inertial force of the particles must be calculated as follows:

$$F_i = -\frac{1}{6}\pi d_p^2\rho_p\frac{du_p}{dt}, \tag{12}$$

where u_p is the velocity of calcium carbonate particles.

2.2.3. Viscous Resistance. When the relative motion of particulate matter occurs in a viscous fluid, there will be momentum transfer, thus subject to viscous drag; the magnitude of drag is determined by the nature of the fluid, the characteristics of the particulate matter, etc. It is generally believed that the drag can be calculated by the following equation:

$$F_d = \frac{\pi}{8}d_p^2C_D\rho\left|u - u_p\right|\left(u - u_p\right), \tag{13}$$

where u is the flow rate of the discharge water, and C_D is the resistance coefficient.

2.2.4. Magnus Force. If there is a velocity gradient in the flow field, the gradient will cause the particles to rotate. In this case, because the pressure on the high-velocity side is low and the pressure on the low-velocity side is high, the resulting differential pressure force will push the sphere toward the high-velocity side, and this pushing force is the Magnus force associated with particle rotation.

2.2.5. Saffman Force. When particles are in a flow field with a velocity gradient, they are subject to transverse lift even if the particles are not rotating. Typically, this force must be considered at the boundary layer due to the large velocity gradient at the wall.

2.2.6. Basset Force. Because the fluid is viscous, the flow field around the particle cannot reach stability immediately when the particle experiences a relative acceleration. Therefore, the force of the fluid on the particle depends not only on the relative velocity of the particle at that time (traction force),

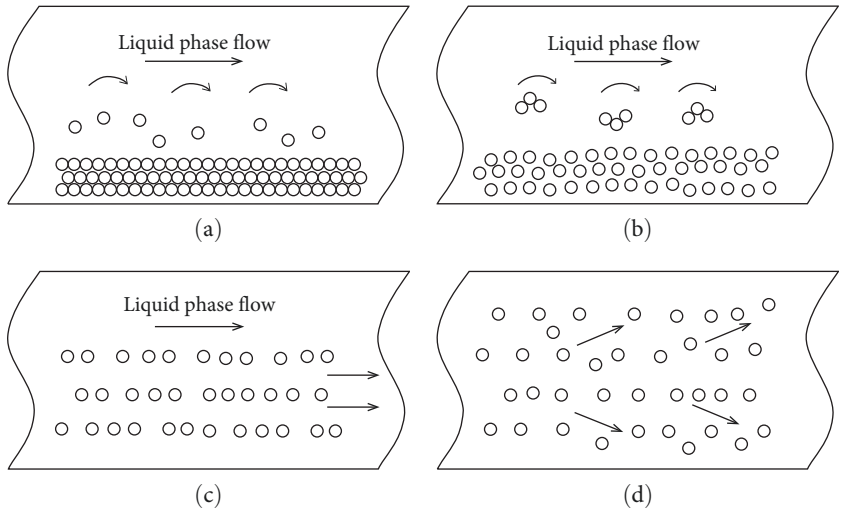

Figure 1: Particle motion states ((a) starting, (b) rolling migration, (c) slipping, and (d) suspended flow).

the relative acceleration at that time (additional inertial force), but also on the history of acceleration before that time, which is related to the changing fluid flow pattern around the calcium carbonate particle.

2.3. Drainage Pipe Granular Flow Pattern Division. The current mainstream school of thought is that as the flow velocity of the liquid phase fluid in the pipe gradually increases, there is a process of solid phase particle movement from initiation to rolling migration followed by slip to suspension flow, as shown in Figure 1.

In order to simplify the calculation model, this paper only for the fourth process of the flow state (Figure 1(d)) for specific analysis; at this time, the liquid phase fluid, after full development to reach a steady state, the entire flow field everywhere the velocity change tends to stabilize, turbulent pulsation phenomenon has been very prominent, the particle phase in the flow field of the vortex area velocity direction change is very violent, when the particle phase in the suspension flow state collision to the wall, there is a certain probability will be captured by the wall.

2.4. Numerical Simulation Modeling. According to the above research on the mechanism of crystallization in tunnel drainage pipes, the influencing factors, and the rate of scaling, as well as the actual research in the field, it can be found that the underground water flow in karst areas in the drainage pipe into the drainage pipe, due to changes in pressure, temperature and other conditions, the solubility of soluble salt ions decreases and turns into a supersaturated solution, generating the driving force of ion crystallization precipitation. When the fluid temperature, pressure (partial pressure of carbon dioxide), flow rate, and flow conditions (pipe type, pipe diameter) and other factors change, or the movement of calcium carbonate particles changes, calcium carbonate particles will gradually migrate to the pipe wall and accumulate to form scale. The normal operation of the tunnel drainage system is affected by easy scaling in pipe sections with large changes in temperature, pressure, and flow rate, as well as in various local components (such as bends, valves, etc.). In order to quantify the process of crystallization and blockage in the tunnel drainage system, this paper considers the construction of a numerical model with coupled multi-physical fields of flow field, concentration field, and chemical reaction field and also combines the data from indoor tests to verify the simulation results.

FLUENT is a mainstream CFD software package based on the finite volume method of a completely unstructured grid, with powerful grid support capability, supporting interface discontinuous grid, mixed grid, dynamic/deformation grid, sliding grid, etc. It also has a gradient algorithm based on grid nodes and grid cells, which can accurately meet the constant or nonconstant flow numerical simulations are performed. By activating the embedded DPM (discrete phase model) in FLUENT software, the movement of calcium carbonate solid particles in the drain is simulated, the coupled multiphysics field numerical model of the scaling rate is established, and the erosion and deposition module in DPM is activated to obtain the deposition of particles in the wall of the pipe, and the scaling is further quantitatively analyzed.

In this paper, the flow field analysis model is first constructed (Figure 2). In karst areas, the rock gap fractures are highly developed, and the groundwater resources are abundant, especially when it is in the rainy season, the water output is even more abundant; meanwhile, in order to simplify the model, it is assumed that the fluid domain is filled with a single fluid (water) and the air phase is ignored, so the model mainly consists of the equations of liquid phase control, particle flow control, and interphase coupling.

2.4.1. Liquid Phase Control Equation and Turbulence Equation. The fluid in the discharge pipe can be considered as incompressible flow with constant density because the parameters such as pressure and temperature do not change much in small time intervals, and the full fluid domain is established based on Euler's method, and the law of motion of the viscous incompressible fluid can be used in the Navier–Stokes equation (N–S equation) in the right-angle

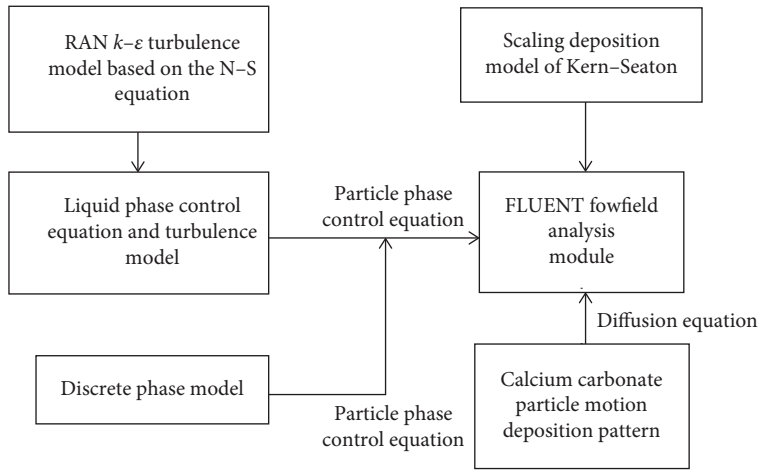

FIGURE 2: Relationship between components of the multiphysics field model.

coordinate system, and its continuous phase equation and N–S equation after the introduction of the law of conservation of momentum and the law of conservation of energy are expressed as follows:

$$\frac{\partial \rho}{\partial t} + \frac{\partial (\rho u_i)}{\partial x_i} = S_{\mathrm{M}}, \tag{14}$$

$$\frac{\partial (\rho u_i)}{\partial t} + \frac{\partial \left(\rho u_i u_j\right)}{\partial x_j} = -\frac{\partial p}{\partial x_i} + \frac{\partial \left(\mu \frac{\partial u_i}{\partial x_j} - \rho \overline{u_i' u_j'}\right)}{\partial x_j} + S_{\mathrm{i}}, \tag{15}$$

$$\frac{\partial (\rho T)}{\partial t} + \frac{\partial (\rho u_i T)}{\partial x_i} = \frac{\partial \left(\frac{k}{C_{\mathrm{p}}} \frac{\partial T}{\partial x_i}\right)}{\partial x_i} + S_{\mathrm{T}}, \tag{16}$$

where ρ is the fluid density, t is time, S_{M} is the source term of the mass equation, mainly related to the production of calcium carbonate particles; p is the pressure on the fluid microelement, μ is the fluid dynamic viscosity, S_{i} is the source term of the momentum equation, mainly related to the momentum transfer between the calcium carbonate particles and the fluid, $u_i u_j$ is the fluid time-averaged velocity component; $u_i' u_j'$ is the fluid pulsation velocity component; C_{p} is the specific heat capacity; S_{T} is the source term of the energy equation, mainly related to the heat transfer between the calcium carbonate particles and the fluid, T is the temperature, k is the thermal conductivity.

Considering that the model is a T-shaped pipe, the main flow pattern is turbulent, and there is a turbulent vortex, the RNA $k-\varepsilon$ model is chosen as the turbulence model. The transport equations related to the turbulent kinetic energy k and dissipation rate ε in this turbulence model are as follows:

$$\frac{\partial (\rho k)}{\partial t} + \frac{\partial (\rho k u_i)}{\partial x_i} = \frac{\partial}{\partial x_j}\left[\alpha_{\mathrm{k}} u_{\mathrm{eff}} \frac{\partial k}{\partial x_j}\right] + G_{\mathrm{k}} + \rho\varepsilon, \tag{17}$$

$$\frac{\partial (\rho \varepsilon)}{\partial t} + \frac{\partial (\rho \varepsilon u_i)}{\partial x_i} = \frac{\partial}{\partial x_j}\left[\alpha_{\varepsilon} u_{\mathrm{eff}} \frac{\partial \varepsilon}{\partial x_j}\right] + \frac{C_{1\varepsilon}^{*} \varepsilon}{k} G_{\mathrm{k}} - C_{2\varepsilon} \rho \frac{\varepsilon^2}{k}, \tag{18}$$

where G_{k} is generated by the turbulent kinetic energy due to the mean velocity gradient, $C_{1\varepsilon}$ and $C_{2\varepsilon}$ are the empirical constant with default values of 1.48 and 1.92, respectively.

2.4.2. Solid–Liquid Two-Phase Flow Coupling Calculation. The volume fraction of the calcium carbonate particle phase is less than 10%, so the DPM model is adopted to simulate the particle phase motion process. For the system containing N particles, to obtain the motion law of the particles, the equations of motion of all the particles must be determined. When the mass of the particles is determined, the equation of motion of the particles is a function of the velocity of each fluid mass around the flow field. Once the coordinates and velocities of the particles are given in the initial model, the positions of the particles at different times and the thermodynamic quantities or other parameters of the system can be calculated based on the laws of classical mechanics. To obtain the relevant fluid parameters at each spatial position of the system, it is necessary to use the Lagrangian model to trace the particle phases and the Eulerian method to describe the flow field, and for solid–liquid two-phase flows, this method solves the continuity and momentum equations for each phase separately, using their associated pressure and other exchange coefficients to achieve coupling of the components.

$$\frac{\partial}{\partial t}(\alpha_b \rho_b) + \nabla \cdot (\alpha_b \rho_b v_b) = \sum_{a=1}^{n} (m_{ab} - m_{ba}) + S_b, \tag{19}$$

$$\begin{aligned} \frac{\partial}{\partial t}(\alpha_b \rho_b v_b) + \nabla \cdot (\alpha_b \rho_b v_b v_b) &= -\alpha_b \nabla p + \nabla \cdot \tau_b + \alpha_b \rho_b g \\ &+ \sum_{b=1}^{n} (R_{ba} + m_{ba} v_{ba} - m_{ab} v_{ab}) \\ &+ \left(F_b + F_{\mathrm{lift},b} + F_{wl,b} + F_{\mathrm{vm},b} + F_{\mathrm{td},b}\right), \end{aligned} \tag{20}$$

where v_b is the velocity of the phase b, m_{ab} is the mass transferred from phase a to phase b, S_b is the source term, τ_b is the stress–strain tensor, g is the gravitational acceleration, R_{ba} is the inter phase force, v_{ab} is the inter phase velocity, F_b is the residual volume force, $F_{\text{lift},b}$ is the buoyancy force, $F_{\text{wl},b}$ is the wall lubrication force, $F_{\text{vm},b}$ is the virtual mass force, and $F_{\text{td},b}$ is the turbulent dissipation force. The above forces are calculated as follows:

$$F_{\text{lift}} = -C_{\text{lift}}\rho_b\alpha_a(\nu_b - \nu_a) \times (\nabla \times \nu_b), \tag{21}$$

$$F_{wl} = -C_{\text{wl}}\rho_b\alpha_a|(\nu_b - \nu_a)_{ll}|^2 n_w, \tag{22}$$

$$F_{\text{vm}} = C_{\text{vm}}\alpha_a\rho_b\left(\frac{d\nu_b}{dt} - \frac{d\nu_a}{dt}\right), \tag{23}$$

$$F_{\text{td,b}} = -F_{\text{td,a}} = -f_{\text{td,lim}}K_{ab}\nu_{\text{dr}}, \tag{24}$$

$$\sum_{b=1}^{n} R_{ba} = \sum_{b=1}^{n} K_{ba}(\nu_b - \nu_a), \tag{25}$$

where C_{lift} is the lift coefficient, C_{wl} is the wall lubrication coefficient, $\left|(\nu_b - \nu_a)_{\|}\right|$ is the relative velocity component of the phase tangent to the wall, n_w is the direction normal to the outer wall, C_{vm} is the imaginary mass coefficient, $f_{\text{td,lim}}$ is other factors limiting the turbulent dissipation force, v_{dr} is the drift velocity, and K_{ba} is the inter phase momentum exchange coefficient.

The energy equation solved by the Euler model is as follows:

$$\begin{aligned}&\frac{\partial}{\partial t}(\alpha_b\rho_b h_b) + \nabla \cdot (\alpha_b\rho_b u_b h_b)\\ &= \alpha_b\frac{\partial p}{\partial t} + \tau_b \cdot \nabla u_b - \nabla \cdot q_b + S_b\\ &\quad + \sum_{a=1}^{n}(Q_{ab} + m_{ab}h_{ab} - m_{ba}h_{ba}),\end{aligned} \tag{26}$$

where q_b is the heat flux of phase b, Q_{ab} is the heat exchange between a and b phases, and h_{ab} is the enthalpy between phases.

For the actual process of calcium carbonate particle deposition, the initial condition of particle release in the DPM model is chosen as a surface jet (surface), the inlet boundary is simultaneously a jet inflow jet surface, and the interaction forces between particles and particles are not considered, and all kinds of forces and heat transfer are considered, but itself will not participate in the reaction because of heat, so its type is set to inert particles.

2.5. Numerical Modeling of Solid–Liquid Two-Phase Flow in Tunnel Drains. A numerical simulation and analysis model of a tunnel drainage pipe chemical crystallization blockage test was established using the finite volume method, and the model was created based on the tunnel drainage pipe axis as the centerline. The numerical analysis is also based on the model test, considering the control of the crystallization rate by the calcium carbonate particle content and hydrodynamic characteristics of the tunnel drainage, and the physical parameters selected in the model, such as water flow velocity, calcium carbonate particle concentration, temperature, and pipe diameter parameters, are consistent with the tunnel drainage pipe in the field.

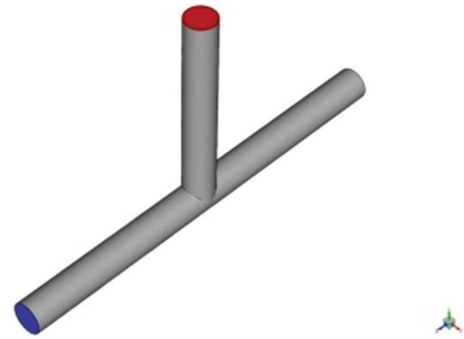

Figure 3: Geometry of drainage pipe model.

According to the field research, it is known that the "T" pipe in the tunnel drainage system is the most clogged place, and the crystallization phenomenon is very obvious here, which is the main part of calcium carbonate particle fouling. Therefore, this paper takes the "T" shaped longitudinal pipe as the simulation object and conducts numerical simulation research to analyze the scaling and clogging process of the drainage pipe under various working conditions. The model pipe material is PVC pipe, the pipe diameter is set to 110 mm, the wall thickness is 4 mm, the length of the horizontal pipe is 1 m, the longitudinal length is 2 m, the end of the horizontal pipe is connected with its T-joint in the middle of the longitudinal pipe, the model ignores the details of the thickness change at the joint, the specific geometric model is shown as Figure 3.

According to the grouping of calcium carbonate precipitation content obtained from chemical crystallization blockage test and hydrochemical software, FLUENT CFD software was used to construct the analysis model of chemical crystallization blockage of tunnel drainage pipe, and the release rate of discrete phase of calcium carbonate was set to 90, 120, 150, 180, and 210 mg/s, respectively, in DPM module, the water flow rate was set to 1, 2, and 3 m/s for numerical analysis. Based on the numerical simulation model of the fouling rate established in the previous paper, FLUENT software is used for the numerical simulation of the fouling process. The boundary conditions to be determined in the simulation include inlet boundary conditions, outlet boundary conditions, and wall conditions, as well as the boundary conditions of the liquid phase and discrete phase.

2.5.1. Boundary Conditions. In order to obtain a unique solution to a physical problem (various differential equations), various parameter values must be set for the computational domain boundaries, such as various fluxes (heat flux, mass flux), motion conditions, etc. At this point, it is necessary to define the information on the location of the boundary conditions (e.g., inlet, solid wall surface, symmetrically located surface) and to determine the information on the various

Table 1: Simulation scheme.

Control variables	Model simulation conditions	Comparative analysis of simulation conditions
Inlet flow rate (m/s)	2	4, 6, 8, 10
Particle flow rate (kg/s)	1×10^{-5}	—
Particle size (μm)	50	100, 200, 400, 800
Temperature (°C)	15	5, 10, 20, 25
Outlet pressure (Pa)	1.01×10^{5}	—

parameters on the boundary. The specific content of the boundary conditions is closely related to the physical model used in the calculation and the type of boundary conditions, which can directly affect the solution process and the results obtained.

(1) Liquid-Phase Flow Field Boundary Conditions. For both ends of the longitudinal pipe, the velocity is used as its boundary control condition, where the inlet velocity of the fluid is defined, and a fully developed turbulent flow and boundary layer are set, with suitable turbulence intensity and hydraulic radius selected.

The boundary condition at the end of the cross pipe is selected as the outflow boundary, set as the pressure outlet, and described by the gauge pressure; the pressure value is the same as the standard atmospheric pressure. The wall boundary condition is selected as the default solid wall without slip condition. The stability of the wall function has a great influence on the calculation results, and a more robust Enhanced model is selected according to the dimensionless wall distance $y+$ less than 30.

(2) DPM Discrete Phase Boundary Conditions. In order to more ideally describe the actual motion of calcium carbonate particles in the flow field, the initial conditions of the DPM model are chosen as a surface jet source, i.e., shot from the surface of the grid where the velocity inlet comes out, the particle type is calcium carbonate particles, their particle properties are set to inert particles, and the density, i.e., heat transfer properties, etc., are kept as default settings, while other parameters, such as particle size, velocity, and mass flux need to be determined in the subsequent processing according to the parametric analysis. Other parameters such as particle size, velocity, mass flux, etc., need to be determined in the subsequent processing based on the parametric analysis. The volume concentration of calcium carbonate particles in each local component is calculated as follows, which is less than 10% and meets the requirements of the DPM model.

$$\alpha = \frac{4m_{\mathrm{p}}}{\pi\rho_{\mathrm{p}}d_{\mathrm{in}}^{2}u_{\mathrm{in}}}\times 100\%, \tag{27}$$

where α is the volume concentration of calcium carbonate particles, m_{p} is the calcium carbonate mass flow rate, u_{in} is the fluid frontal inlet flow rate, and d_{in} is the diameter of the pipe inlet face.

Since the model simulates the deposition of calcium carbonate particles on the pipe wall, the wall conditions of the DPM model are set to capture the boundary.

2.5.2. Model Parameter Setting. The influencing factors such as inlet flow velocity, particle concentration, and particle size were selected as the study factors, and the influence of temperature on the flow field and calcium carbonate particle movement was ignored due to the relatively small length of the drain pipe and the small temperature change, and the flow field velocity was uniformly set at 15°C.

(1) Simulated Inlet Flow Rate Selection. According to the highway drainage design specifications and local hydrological data, as well as the actual operation of the drainage pipe, the main selection of fluid inlet velocity of 5 m/s for simulation studies, and another selection of flow velocity of 4, 6, 8, 10 m/s for comparative analysis.

(2) Selection of Total Flow Rate of Calcium Carbonate Particles. According to the calculation of PHREEQC chemical reaction software, the release flow rate of calcium carbonate in the DPM module was set to 1×10^{-5} kg/s by combining with the actual test data.

(3) Particle Size Selection. The diameter of calcium carbonate particles is directly related to their flow characteristics in the flow field; according to previous studies, large particles are more likely to precipitate, small particles are more likely to adsorb on the pipe wall, and small calcium carbonate particles are likely to attract each other to form larger particles, so set the particle diameter of 50, another 100, 200, 400, 800 μm were selected for comparative studies, calcium carbonate particles initial velocity is zero.

(4) Specific Simulation Scenarios. Based on the above analysis, the specific calcium carbonate crystallization simulation scheme for the T-pipe section of the drainage pipe is derived, as shown in Table 1.

For calcium carbonate particles moving in each local component, the deposition rate φ_{dep} is an important parameter for examining the rate of fouling as well as the amount of fouling:

$$\varphi_{\mathrm{dep}} = \frac{N_{\mathrm{trap}}}{N_{\mathrm{trap}}+N_{\mathrm{escape}}}\times 100\%, \tag{28}$$

where N_{trap} is the number of calcium carbonate particles captured (deposited) by the drain pipe wall and N_{escape} is the number of calcium carbonate escaping from the outlet.

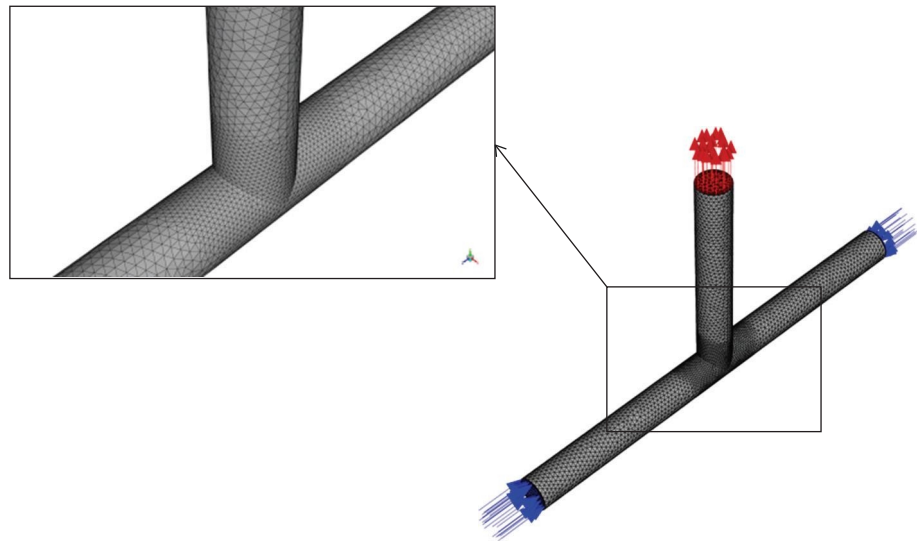

Figure 4: Grid division.

Actual mass fraction of calcium carbonate deposition,

$$m_f = m_p \times \varphi_{\text{dep}}, \tag{29}$$

where m_f is the actual calcium carbonate mass fraction and m_p is the mass fraction of calcium carbonate produced.

2.5.3. Model Meshing. According to the geometric model of the drainage pipe in Figure 3, the pipe is meshed using the scanning meshing method (sweep) and divided into a hexahedral structure mesh, with a total of 122,689 meshes, 272,679 mesh faces, 37,963 nodes, and local encryption is set at the intersection of the longitudinal and transverse pipes, while the boundary layer mesh is divided according to the wall function, and the number of boundary layers is The number of boundary layers is five, and the model grid is shown below. The direction of gravity in the model is along the positive direction of the x-axis, the arrow marks the boundary conditions, the red arrow is the outlet boundary, the blue arrow is the inlet boundary, the fluid flows along the y-axis, and the direction is perpendicular to the inlet boundary. The grid division details are shown in Figure 4.

2.6. Indoor Test Verification. To ensure the real validity of the DPM granular flow numerical model, conducting field tests is an essential step. The experiments first identified the composition of water samples collected at the site, determined the ionic concentration of each groundwater component, comprehensively analyzed the main groundwater chemical types causing crystalline blockage in the tunnel drainage system, and based on the test results of water samples in the tunnel drainage system, prepared similar simulated solutions (all external conditions were consistent with the numerical model, the concentration of each substance is shown in Table 1), Then, calcium carbonate powder (released by the hourglass) was added to the mixed solution at a rate of 36 g/hr, only the addition rate of the inlet calcium carbonate solids was kept constant, the temperature, inlet flow rate, and calcium carbonate powder particle size of the pipe flow field were changed one by one, and the process of calcium carbonate fouling in the pipe section was reduced by allowing the solution to circulate internally in the indoor simulation test apparatus, and the amount of calcium carbonate scaling was determined by weighing the pipe section after it was dried in an oven.

2.6.1. Test Program. Combined with the numerical simulation scheme and the actual conditions of the engineering site, the test scheme is consistent with Table 2; the standard conditions of the test are flow rate 2 m/s (±0.5 m/s), fluid temperature 15°C (±2°C), calcium carbonate powder mesh is 300 mesh, the control group flow rate is 4, 6, 8, 10 m/s, the temperature is 5, 10, 20, 25°C (with ice and heating rod control), calcium carbonate powder mesh was selected as 160, 75, 36, and 22 mesh, respectively, and only a single variable was controlled for the control experiment, and the rest was determined according to the standard conditions, and each group took 24 hr.

2.6.2. The Configuration of the Test Solution. As calcium carbonate is extremely insoluble in water, the addition of calcium carbonate particles will not change the concentration of various ions in the test solution; the reagents used in the configuration of the solution are mainly anhydrous $CaCl_2$, anhydrous Na_2CO_3, $NaHCO_3$, $MgCl–6H_2O$ and anhydrous sodium sulfate produced by Sinopharm Chemical Reagent Company for configuration (Figure 5), the test water is 60-L deionized water, add the appropriate amount of reagents to make various ions to the specified concentration.

2.6.3. Construction of the Test Model. The test pipe is made of PVC water pipe with a diameter of 110 mm, cut into a T-shaped pipe section (removable), and the slope of the cross pipe is 3%. The base device consists of two acrylic water tanks of 300 × 300 × 400 mm connected by PVC water pipes of 50 mm diameter (with filter paper inside to filter out calcium carbonate powder) to carry the test solution; the test PVC

Table 2: Parameters of each group of the experimental model.

	Equipment	Model	Quantity	Parameters
Experimental module	Acrylic tank	Plexiglass	2	30 × 30 × 40
	Water pump	XQP-2500	1	80 W
	PVC pipe	Φ110	50	1 m
	PVC pipe	Φ50	1	1 m
	PVC elbow	Φ110	2	—
	PVC tee connector	Φ110	15	—
Measuring instruments	Electronic balance	YINGHENG	1	Precision 0.01 g
	pH meter	PH848	2	Ph range 0.0–14.0
	Oven	101–3AB	1	Temperature 60°C
	Infrared thermometer	SATA	1	Range −50 to 580°C
	Heating rod	PTC	1	Range 20–100°C

Figure 5: Configure the chemical reagent of the test solution.

Figure 6: Model test materials.

pipes are cut and connected by glue to ensure the same size of the test device, the lid of the carrying box is connected to the pump by 20 mm pipes, the pump is placed inside the base tank. The water pump is placed in the base tank, the test solution in the base tank enters the T-pipe section through the pump, and calcium carbonate powder is added at the same time; the water flows through the T-pipe and finally flows into the base tank, so as to achieve the circulation of the water body. The experimental materials and setup are shown in Figures 6 and 7. Model as shown in Figure 8, the test equipment-related parameters are shown in Table 2.

2.6.4. Acquisition of Experimental Results. The net weight of the test pipe sections of each temperature group was weighed before the start of the test, and each group was run for 24 hr. The weight of the test pipes was recorded, and the mass of the crystalline material was extrapolated during the test, and the pipes were dried at 70°C using a dryer before each measurement in order to ensure the accuracy of the test data (Figure 9). The mass difference was recorded, and the mass fraction of calcium carbonate deposition (the ratio of the amount of fouling to the amount of calcium carbonate powder added) was calculated.

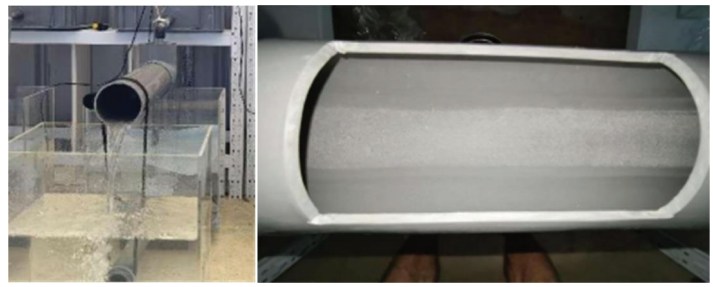

Figure 7: Experimental setup and its observation holes.

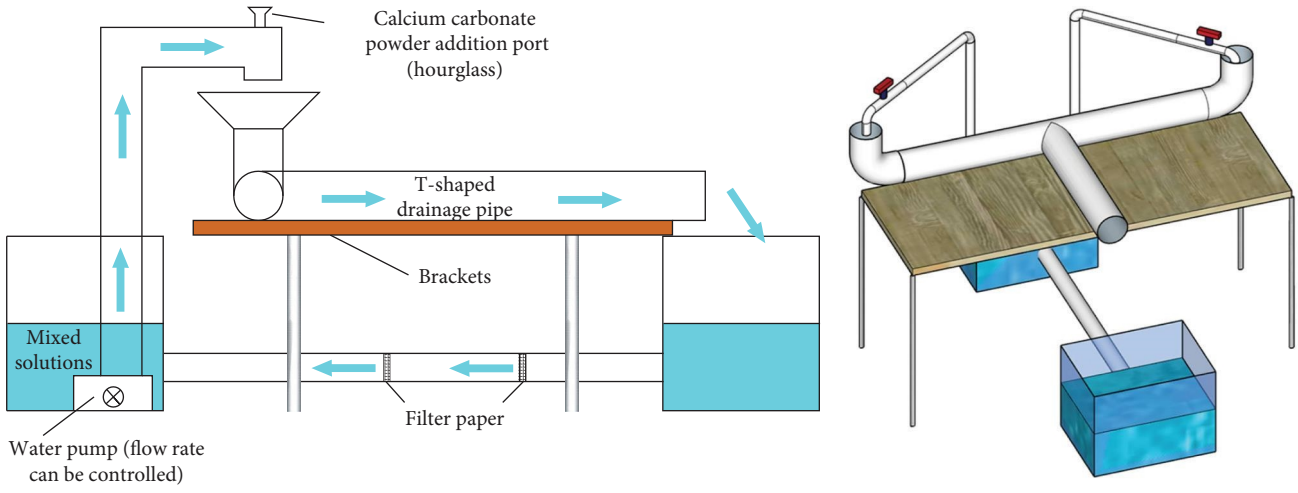

Figure 8: Conceptual diagram of the experimental setup. (a) Plan view of the component cycle and (b) 3D schematic of the experimental model.

Figure 9: Pipe drying and weighing.

3. Results and Discussion

3.1. Comparison of Numerical Model Results with Experimental Results. In order to analyze the effect of the variation of each parameter on the deposition of calcium carbonate particles in the effluent and also to verify the correctness of the deposition proportional rate model by comparing the results of the indoor tests, the flow field temperature, particle size, and inlet flow rate were investigated. Dashed line plots of calcium carbonate mass fraction versus variables were plotted in the indoor tests and numerical models using inlet flow rate, flow field temperature, and particle size as single control variables, respectively, with the following results.

The above figures show the data of calcium carbonate deposition in the pipe section within 24 hr, and the test results and numerical simulation results fit relatively well, which confirms the reliability of numerical simulation. When the experimental variable is temperature, the test result value is generally smaller than the numerical simulation result, probably because the numerical simulation does not consider the external convection, while the field experiment is difficult to ensure the constant water temperature and the actual temperature will be cooled down by convection when the water flows through the pipe, thus affecting the scaling rate.

3.2. Discussion of Parametric Analysis

3.2.1. Inlet Flow Velocity. As shown in Figure 10, if other parameters remain unchanged, it can be seen that the mass fraction of calcium carbonate deposition decreases with the increase of flow velocity, and the laminar effect is stronger than the turbulent effect in the case of low flow velocity, so the particle phase is mainly suspended and migrated in the flow field, and then deposited by gravity; and as the flow velocity gradually increases, the turbulence phenomenon of the particle phase becomes more and more obvious, and the flow line also begins to become disordered, and the fluid in the pipe has a greater carrying effect on the calcium carbonate particles, and even if deposition occurs, it is easier to

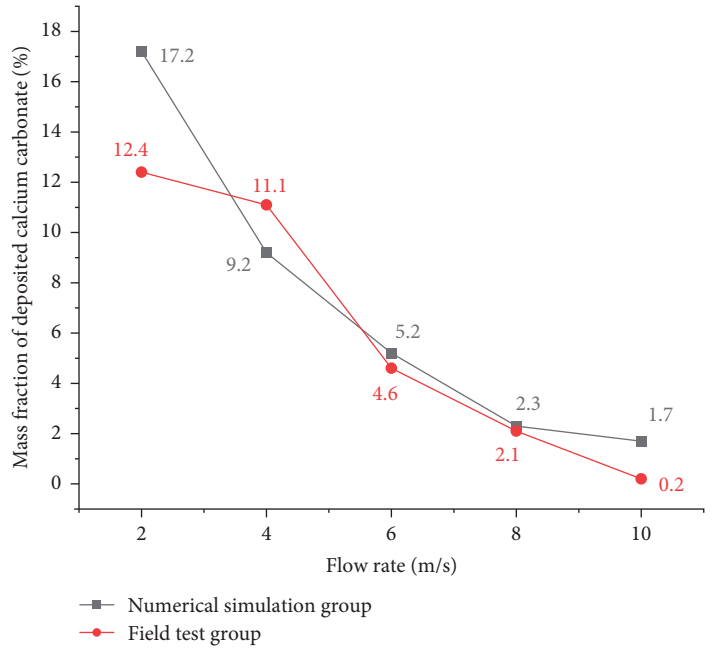

Figure 10: Deposited calcium carbonate mass fraction versus inlet flow rate (comparison).

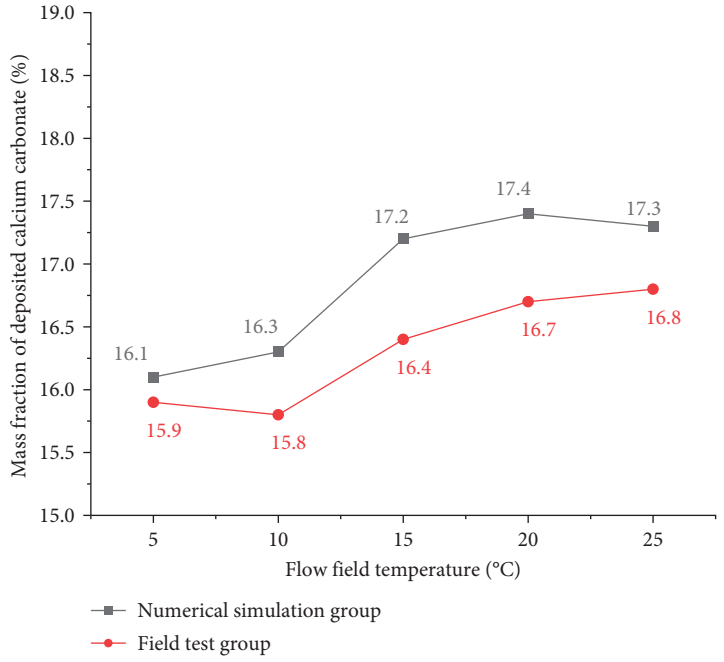

Figure 11: Deposited calcium carbonate mass fraction as a function of fluid temperature (comparison).

scour the already deposited particles, and the particles are more easily washed away by the water flow.

3.2.2. Pipe Section Temperature. From the vertical axis of Figure 11, the effect of temperature on the deposition of calcium carbonate particles is not significant, and the maximum variation of the mass fraction does not exceed 1.2%, which is mainly because the model ignores the effect of temperature on the solubility of calcium carbonate and only considers the effect of temperature on the flow characteristics of the flow field, and also indicates that the temperature has little effect on the movement of calcium carbonate particles at the micron scale.

3.2.3. Particle Diameter. Figure 12 shows that the increase in particle size can significantly increase the mass fraction of deposited calcium carbonate; the particle diameter is directly related to the mass of individual particles; the heavier the calcium carbonate particles, the greater the inertial force, the trapping force also increases with the increase in volume, so

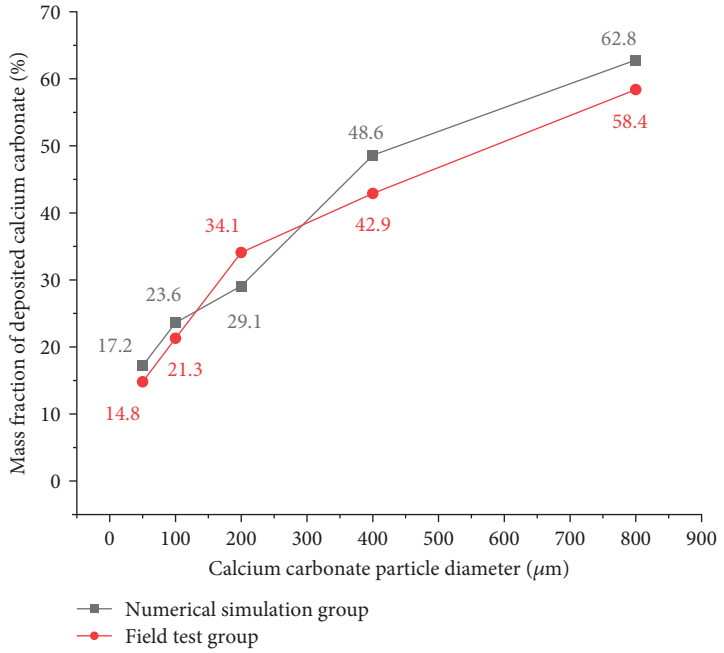

Figure 12: Deposited calcium carbonate mass fraction versus particle size (comparison).

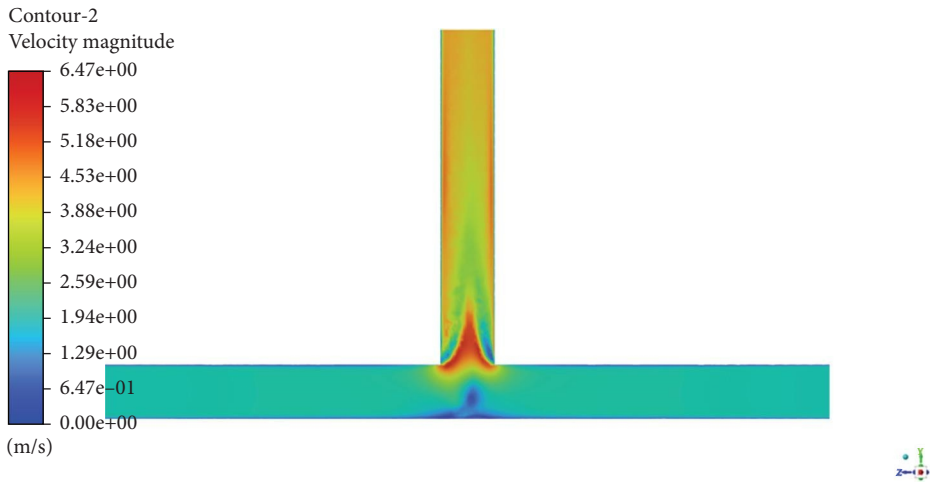

Figure 13: Nephogram of velocity distribution.

the motion of the particle phase in the flow field becomes less and less active, the easier it is to deposit down to be captured by the wall.

3.3. Flow Field Analysis of Numerical Simulation. Calculations were run using FLUENT software with a fluid inlet velocity of 2 m/s and a temperature of 15°C. The results were obtained when the flow developed to a steady state, as shown below.

From the nephogram of velocity distribution (Figure 13) and nephogram of steady pressure distribution (Figure 14) can be seen when the water flow from the two ends of the longitudinal pipe relative inflow, fluid successively into the horizontal pipe, the fluid velocity at the top of the horizontal pipe reached the maximum, T-type interface at the center of the velocity maximum, 3.35 times the inlet velocity, reached 6.7 m/s, while the pressure value decreases sharply, and quickly converge to the atmospheric pressure value. In the flow layer near the wall, due to the constraints of the wall, the fluid mass basically can not move perpendicular to the direction of the wall; the viscous shear stress plays a dominant role, the fluid velocity will be reduced, while the closer the wall, the greater the flow velocity gradient, indicating that the fluid velocity in the near-wall area changes more drastically. According to the continuity equation, when the fluid velocity at the boundary layer of the wall decreases, its corresponding other fluid velocity will increase accordingly, and due to the role of fluid viscosity, the accelerated fluid will drive the fluid at the boundary layer, making the appearance of the parametric pressure gradient at the wall.

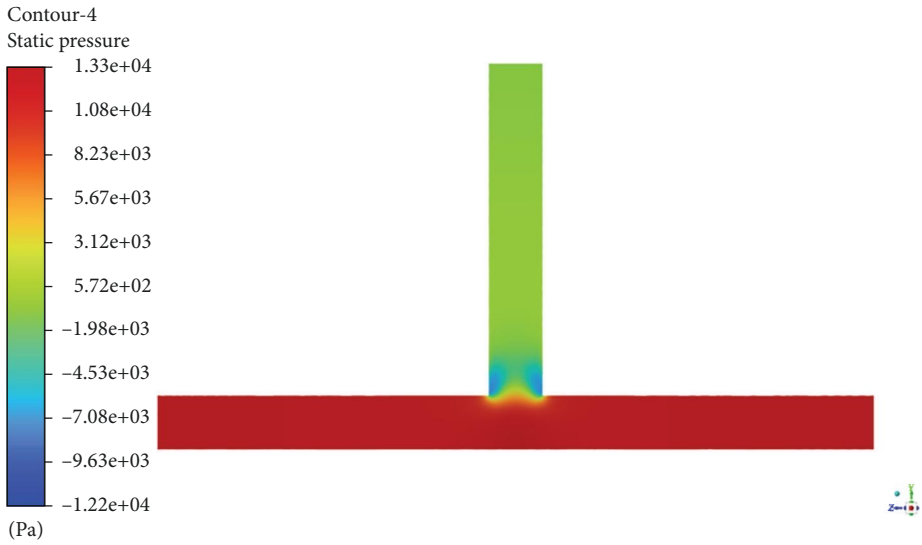

Figure 14: Nephogram of steady-state pressure distribution.

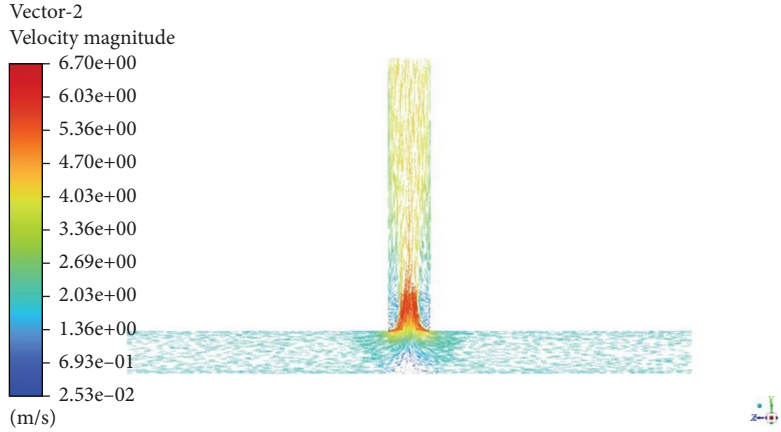

Figure 15: Streamline vector drawing.

In the T-pipe wall, the details of the vector diagram (Figures 15 and 16) show that the flow field here appears vortex, the flow velocity is small, and the pressure is low; the flow line shows the phenomenon of intersection with the pipe wall, so it can first be inferred that the introduction of DPM model calcium carbonate particles are easy to accumulate and adsorption here, but the central position of the pipe here is the largest flow velocity. However, the flow velocity in the center of the pipe is the largest, and the calcium carbonate particles accumulated here are subjected to a greater scouring effect, which is likely to carry away the calcium carbonate particles, resulting in the content of calcium carbonate in the center of the pipe may be more than the content of the pipe wall.

3.4. Analysis of the Phase Motion Law of Calcium Carbonate Particles. The DPM particle phase analysis model is established, and the software automatically couples calcium carbonate as a discrete phase with the liquid phase flow field in one direction and calculates the motion of particles in the fluid domain according to the flow field characteristics and calculation results, and records their trajectories, motion speed, residence time, wall capture results and other information.

When the temperature is 15°C, the inlet flow rate is 2 m/s, and the particle diameter is 50 μm, the calcium carbonate in the drain is discrete into 174 spherical particles in total, and the following figure shows the specific trajectory of particle movement.

Figures 17 and 18 show the residence time and velocity data of calcium carbonate particles in the flow field. The particle phase moves with the flow field, and the velocity distribution law is basically the same as the flow field, and the residence time distribution law is inversely related to the velocity distribution. It can be seen that when the particle phase moves in the longitudinal pipe, the motion of calcium carbonate particles is basically the same, but from the T-shaped interface into the horizontal pipe, the turbulence effect is obvious, and the angle of the particles at the interface is very large. Therefore, the wall at the end of the cross pipe is the main area for particle deposition, and the capture of particles by the wall is likely to occur there.

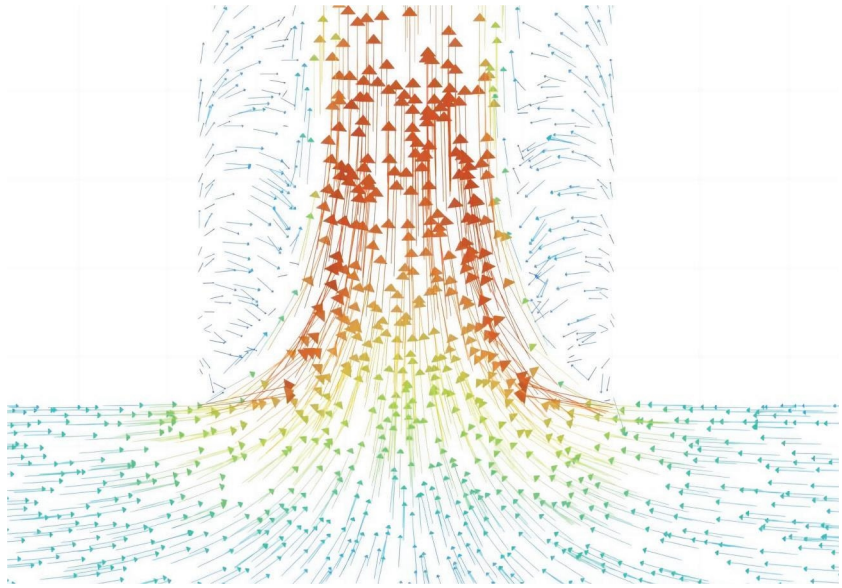

Figure 16: Detail of vector drawing at T-junction.

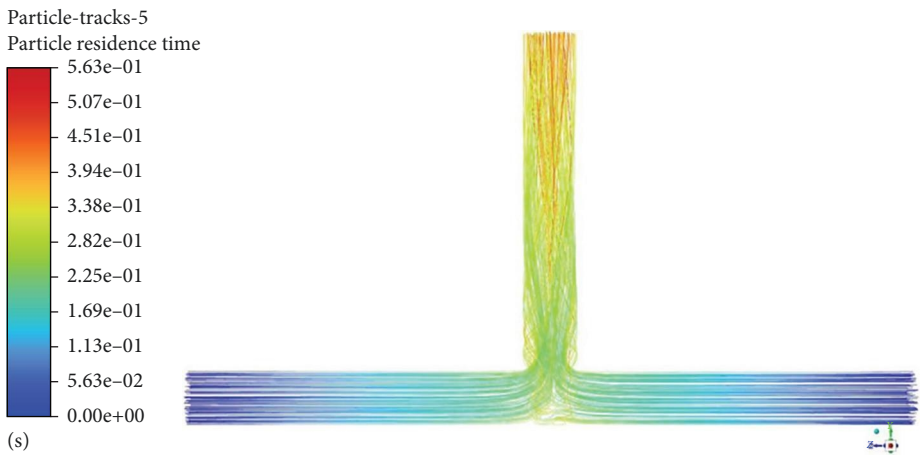

Figure 17: Particle motion trajectory (colors represent residence time).

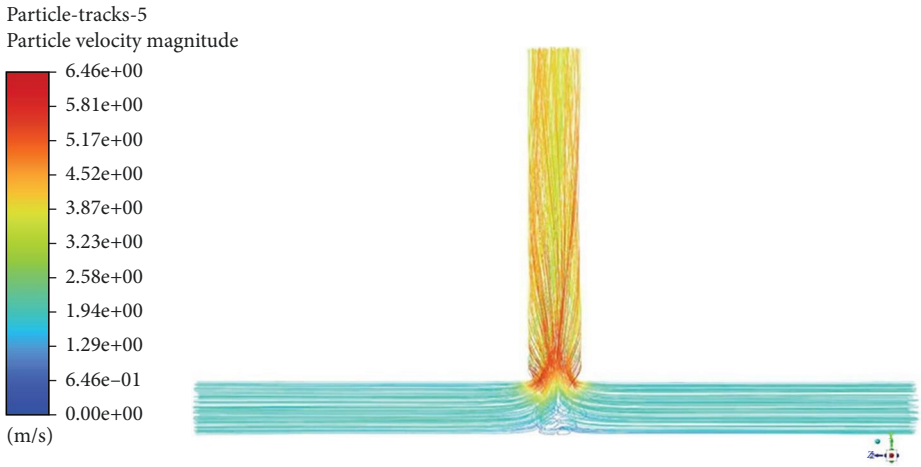

Figure 18: Particle trajectory (colors represent velocity).

According to the calculated results, this simulation showed that a total of 4 out of 174 particles were captured by the wall, and the deposition rate obtained after conversion, according to Equation (28), was 2.3%.

4. Conclusions

This paper studies and analyzes the process of calcium carbonate scale formation and the force of particle phase in the drainage pipe, provides theoretical basis for the analysis of crystallization blockage mechanism and numerical simulation model of tunnel drainage pipe in karst areas, and establishes a numerical analysis of calcium carbonate particle deposition rate of drainage pipe considering the coupling of solid–liquid two-phase flow based on FLUENT hydrodynamic simulation software, using DPM discrete phase particle flow model. At the same time, field experiments were conducted, and the simulation results were compared with the field experimental results for verification to ensure the reliability of the numerical model. The specific conclusions were as follows:

(1) In the flow field simulation of FLUENT software, the specific flow characteristics of the fluid in the pipe and the spatial distribution law of parameters such as flow velocity and pressure are obtained, and the trajectory of the calcium carbonate particle phase in the flow field can be clearly seen, and the correlation between the scaling effect and fluid velocity, flow field temperature and scale particle diameter is obtained.

(2) For different flow environments, the deposition rate of calcium carbonate particles is different, and the distribution of its deposition on the pipe wall is also different due to the scouring effect of the fluid, and the main deposition location of calcium carbonate is mainly concentrated at the T-junction of the drain pipe, i.e., at the end of the cross pipe. With the temperature, flow rate, particle diameter will affect the amount of calcium carbonate deposition scaling; particle diameter has the greatest impact on the mass fraction of its deposition; the larger the particles in the process of flow, the more likely to occur in the pipe wall deposition of scaling phenomenon.

(3) The method proposed in this paper can also provide ideas to accurately predict the amount of scale crystallization and scale treatment in drains, such as controlling the change of pipe wall roughness coefficient to increase the flow rate or using physicochemical means to prevent the growth of nuclei. The flow field distribution at the entrance of the drainage pipe is also worthy of discussion. This model does not consider the influence of foam geotextile or mortar on groundwater seepage in the tunnel waterproof layer [32, 33]. If these factors are added, more useful conclusions may be obtained.

Data Availability

The data used to support the findings of this study are available upon request from the corresponding author (ljb@gdut.edu.cn).

Conflicts of Interest

The authors declare that they have no conflicts of interest.

Acknowledgments

This research was supported by the following projects: the National Natural Science Foundation of China Youth Fund Project "Research on the vertical bearing mechanism and design calculation method of foundation piles in multi-karst cave strata (no. 52108316)" and the Guangdong Provincial Outstanding Youth Fund Project "Research on the bearing mechanism and stability of pile foundation in karst areas based on static and dynamic loads and time-varying soil properties (no. 2023B1515020061)."

References

[1] Z. Zhuo, *Research on mechanism of groundwater seepage and crystallization blocking tunnel drainage pipe in karst areas and treatment suggestions*, M.A. thesis, Chang'an University, 2015.

[2] G. Kelling and P. R. Mullin, "Graded limestones and limestone-quartzite couplets: possible storm-deposits from the Moroccan carboniferous," *Sedimentary Geology*, vol. 13, no. 3, pp. 161–190, 1975.

[3] J. W. Morse, "Dissolution kinetics of calcium carbonate in sea water; V, effects of natural inhibitors and the position of the chemical lysocline," *American Journal of Science*, vol. 274, no. 6, pp. 638–647, 1974.

[4] L. N. Plummer, T. M. L. Wigley, and D. L. Parkhurst, "The kinetics of calcite dissolution in CO_2–water systems at 5 degrees to 60 degrees C and 0.0 to 1.0 atm CO_2," *American Journal of Science*, vol. 278, no. 2, pp. 179–216, 1978.

[5] F. Brahim, W. Augustin, and M. Bohnet, "Numerical simulation of the fouling process," *International Journal of Thermal Sciences*, vol. 42, no. 3, pp. 323–334, 2003.

[6] J. E. Oddo and M. B. Tomson, "Why scale forms in the oil field and methods to predict it," *SPE Production & Facilities*, vol. 9, no. 1, pp. 47–54, 1994.

[7] F. Brahim, W. Augustin, and M. Bohnet, "Numerical simulation of the fouling on structured heat transfer surfaces (fouling)," in *Heat Exchanger Fouling and Cleaning: Fundamentals and Applications*, pp. 1–9, ECI Digital Archives, 2003.

[8] M. Nergaard, R. Beck, M. Seiersten, and J.-P. Andreassen, "Scaling of calcium carbonate on the exterior of heated surfaces in a flow-through setup," *Chemical Engineering & Technology*, vol. 37, no. 8, pp. 1321–1328, 2014.

[9] J. Fang, B. Jiao, G. Zhao, L. He, Y. Wu, and C. Dai, "Study on the channel flow control regulation of particle agents in fractured-vuggy carbonate reservoirs via CFD-DEM coupling method," *Journal of Petroleum Science and Engineering*, vol. 180, pp. 495–503, 2019.

[10] Chi, Lan, and Xiao, "Effects of solution temperature and CO_2 content on the solubility of feldspar," *Journal of Water*

Resources and Hydraulic Engineering, vol. 25, no. 2, pp. 230–232, 2014.

[11] R. de Paula Cosmo, F. de Assis Ressel Pereira, E. J. Soares, and A. Leibsohn Martins, "Modeling and validation of the CO_2 degassing effect on $CaCO_3$ precipitation using oilfield data," *Fuel*, vol. 310, Part B, Article ID 122067, 2022.

[12] X. Zhiming, Z. Jinchao, Z. Zhongbin, and B. Shan, "Crystallization fouling model and numerical simulation of $CaSO_4$ in tube," *Chemical Engineering*, (07): 13-16. (In Chinese), 2009.

[13] Z. Liu, H. Onay, F. Guo, Q. Lv, and E. J. R. Sudhölter, "Real-time monitoring of electrochemically induced calcium carbonate depositions: kinetics and mechanisms," *Electrochimica Acta*, vol. 370, Article ID 137719, 2021.

[14] T. Chen, S. Honarparvar, D. Reible, and C.-C. Chen, "Thermodynamic modeling of calcium carbonate scale precipitation: aqueous Na+-Ca2+-Cl−-HCO_3−-CO_{32}−-CO_2 system," *Fluid Phase Equilibria*, vol. 552, Article ID 113263, 2022.

[15] U. Ojaniemi, T. Pättikangas, A. Jäsberg, E. Puhakka, and A. Koponen, "Computational fluid dynamics simulation of fouling of plate heat exchanger by phosphate calcium," *Heat Transfer Engineering*, vol. 43, no. 15-16, pp. 1396–1405, 2022.

[16] C. Guanying and H. Jixiang, "Traceability analysis of Ca∼(2+) in aqueous solution behind the curtain in the dam site area," *People's Yellow River*, vol. 44, no. S1, pp. 77–79, 2022.

[17] Zhao, "Numerical simulation of fouling characteristics of leachate transport pipeline based on CFD," *Environmental Engineering*, vol. 41, no. 3, pp. 111–11, 2023.

[18] Y. Lü, K. Lu, Y. Bai, Y. Ma, and Y. Ren, "Fouling characteristics of 90° elbow in high salinity wastewater from coal chemical industry," *Chinese Journal of Chemical Engineering*, vol. 35, pp. 143–151, 2021.

[19] C. W. Turner and D. W. Smith, "Calcium carbonate scaling kinetics determined from radiotracer experiments with calcium-47," *Industrial & Engineering Chemistry Research*, vol. 37, no. 2, pp. 439–448, 1998.

[20] S. Ciukaj and B. Hernik, "Field and CFD study of fuel distribution in pulverized fuel (PF) boilers," *Journal of Thermal Science*, vol. 29, pp. 535–545, 2020.

[21] J. Ma, J. Chen, W. Chen, and L. Huang, "A coupled thermal-elastic-plastic-damage model for concrete subjected to dynamic loading," *International Journal of Plasticity*, vol. 153, Article ID 103279, 2022.

[22] J. Ma, J. Chen, J. Guan, Y. Lin, W. Chen, and L. Huang, "Implementation of Johnson–Holmquist–Beissel model in four-dimensional lattice spring model and its application in projectile penetration," *International Journal of Impact Engineering*, vol. 170, Article ID 104340, 2022.

[23] X. Xu, Y. Zhang, L. Li, and C.-B. Xu, "Model test on crystallization law of tunnel drainage pipe in karst area," *Highway Traffic Science and Technology*, vol. 39, no. 2, pp. 133–139, 2022.

[24] W. Zhou, Y. Wang, Y. Li, L. Wang, and X. Jia, "Experimental study on the factors influencing the crystallization and precipitation hydrodynamics of tunnel drainage pipes in karst areas," *Highway*, vol. 66, no. 3, pp. 347–352, 2021.

[25] R. S. Feng, J. Zhou, D. Xiao, X. Chen, H. Li, and X. Zhang, "Indoor experimental study on crystallization growth of tunnel drainage pipe in high geothermal zone," *Highways*, vol. 66, no. 9, pp. 398–402, 2021.

[26] A. Neville and A. P. Morizot, "A combined bulk chemistry/electrochemical approach to study the precipitation, deposition and inhibition of $CaCO_3$," *Chemical Engineering Science*, vol. 55, no. 20, pp. 4737–4743, 2000.

[27] V. Kannojiya, S. Kumar, M. Kanwar, and S. K. Mohapatra, "Simulation of erosion wear in slurry pipe line using CFD," in *Mechanical Engineering Design*, pp. 459–465, Trans Tech Publications Ltd., 2016.

[28] M. H. Zolfagharnasab, M. Salimi, H. Zolfagharnasab, H. Alimoradi, M. Shams, and C. Aghanajafi, "A novel numerical investigation of erosion wear over various 90-degree elbow duct sections," *Powder Technology*, vol. 380, pp. 1–17, 2021.

[29] P. Kjellin, K. Holmberg, and M. Nydén, "A new method for the study of calcium carbonate growth on steel surfaces," *Colloids and Surfaces A: Physicochemical and Engineering Aspects, 2001*, vol. 194, no. 1–3, pp. 49–55, 2001.

[30] D. Kern and R. Seaton, "A theoretical analysis of thermal surface fouling," *British Chemical Engineering*, vol. 4, no. 5, pp. 258–262, 1959.

[31] M. Bohnet, "Fouling of heat transfer surfaces," *Chemical Engineering & Technology*, vol. 10, no. 1, pp. 113–125, 1987.

[32] J. Ma, J. Chen, W. Chen, C. Liu, and W. Chen, "A bounding surface plasticity model for expanded polystyrene-sand mixture," *Transportation Geotechnics*, vol. 32, Article ID 100702, 2022.

[33] J. Ma, J. Guan, Y. Gui, and L. Huang, "Anisotropic bounding surface plasticity model for porous media," *International Journal of Geomechanics*, vol. 21, no. 4, 2021.